Identification of a novel potassium channel (GiK) as a potential drug target in *Giardia lamblia*: Computational descriptions of binding sites

Lissethe Palomo-Ligas [1], **Filiberto Gutiérrez-Gutiérrez** [2], **Verónica Yadira Ochoa-Maganda** [1], **Rafael Cortés-Zárate** [3], **Claudia Lisette Charles-Niño** [3], **Araceli Castillo-Romero** Corresp. [3]

[1] Departamento de Fisiología, Centro Universitario de Ciencias de la Salud, Universidad de Guadalajara, Guadalajara, Jalisco, Mexico

[2] Departamento de Química, Centro Universitario de Ciencias Exactas e Ingenierías, Universidad de Guadalajara, Guadalajara, Jalisco, Mexico

[3] Departamento de Microbiología y Patología, Centro Universitario de Ciencias de la Salud, Universidad de Guadalajara, Guadalajara, Jalisco, Mexico

Corresponding Author: Araceli Castillo-Romero
Email address: araceli.castillo@cucs.udg.mx

Background. The protozoan *Giardia lamblia* is the causal agent of giardiasis, one of the main diarrheal infections worldwide. Drug resistance to common antigiardial agents and incidence of treatment failures have increased in recent years. Therefore, the search for new molecular targets for drugs against *Giardia* infection is essential. In protozoa, ionic channels have roles in their life cycle, growth, and stress response. Thus, they are promising targets for drug design. The strategy of ligand-protein docking has demonstrated a great potential in the discovery of new targets and structure-based drug design studies. **Methods.** In this work, we identify and characterize a new potassium channel, GiK, in the genome of *Giardia lamblia.* Characterization was performed *in silico.* Because its crystallographic structure remains unresolved, homology modeling was used to construct, the three-dimensional model for the pore domain of GiK. The docking virtual screening approach was employed to determine whether GiK is a good target for potassium channel blockers. **Results.** The GiK sequence showed 24-50% identity and 50-90% positivity with 21 different types of potassium channels. The quality assessment and validation parameters indicated the reliability of the modeled structure of GiK. We identified one hundred ten potassium channel blockers exhibiting high affinity toward GiK. Thirty-nine of these drugs bind in three specific regions. **Discussion.** The GiK pore signature sequence is related to the small conductance calcium-activated potassium channels (SKCa). The predicted binding of one hundred ten potassium blockers to GiK makes this protein an attractive target for biological testing to evaluate its role in the life cycle of *Giardia lamblia* and potential candidate for the design of novel antigiardial drugs.

Identification of a novel potassium channel (GiK) as a potential drug target in *Giardia lamblia*: Computational descriptions of binding sites.

Lissethe Palomo-Ligas[1], Filiberto Gutiérrez-Gutiérrez[2], Verónica Yadira Ochoa-Maganda[1], Rafael Cortés-Zárate[3], Claudia Lisette Charles-Niño[3], Araceli Castillo-Romero[3]

[1]Departamento de Fisiología, Centro Universitario de Ciencias de la Salud, Universidad de Guadalajara, Guadalajara Jalisco, México

[2]Departamento de Química, Centro Universitario de Ciencias Exactas e Ingenierías, Universidad de Guadalajara, Guadalajara, Jalisco, México

[3]Departamento de Microbiología y Patología, Centro Universitario de Ciencias de la Salud, Universidad de Guadalajara, Guadalajara Jalisco, México

Corresponding author

Araceli Castillo-Romero[3]

E-mail: araceli.castillo@cucs.udg.mx

Abstract

Background. The protozoan *Giardia lamblia* is the causal agent of giardiasis, one of the main diarrheal infections worldwide. Drug resistance to common antigiardial agents and incidence of treatment failures have increased in recent years. Therefore, the search for new molecular targets for drugs against *Giardia* infection is essential. In protozoa, ionic channels have roles in their life cycle, growth, and stress response. Thus, they are promising targets for drug design. The strategy of ligand-protein docking has demonstrated a great potential in the discovery of new targets and structure-based drug design studies.

Methods. In this work, we identify and characterize a new potassium channel, GiK, in the genome of *Giardia lamblia.* Characterization was performed *in silico.* Because its crystallographic structure remains unresolved, homology modeling was used to construct, the three-dimensional model for the pore domain of GiK. The docking virtual screening approach was employed to determine whether GiK is a good target for potassium channel blockers.

Results. The GiK sequence showed 24-50% identity and 50-90% positivity with 21 different types of potassium channels. The quality assessment and validation parameters indicated the reliability of the modeled structure of GiK. We identified one hundred ten potassium channel blockers exhibiting high affinity toward GiK. Thirty-nine of these drugs bind in three specific regions.

Discussion. The GiK pore signature sequence is related to the small conductance calcium-activated potassium channels (SKCa). The predicted binding of one hundred ten potassium blockers to GiK makes this protein an attractive target for biological testing to evaluate its role in the life cycle of *Giardia lamblia* and potential candidate for the design of novel antigiardial drugs.

1. Introduction

Giardia lamblia is the causal agent of giardiasis, a prolonged diarrheal disease. The standard compounds used against *Giardia lamblia* are 5-nitroimidazoles. However, these compounds present side effects associated with residual toxicity in the host.

Dose-dependent side effects include leukopenia, headache, vertigo, nausea, insomnia, irritability, metallic taste, and CNS toxicity (Ansell et al. 2015; Escobedo & Cimerman 2007; Tejman-Yarden & Eckmann 2011; Watkins & Eckmann 2014). In addition, reports of resistant strains and nitroimidazole-refractory disease are of considerable concern. Reduced efficacy has been described even with higher drug doses (Carter et al. 2018; Leitsch 2015). For these reasons, there is a significant need for identification of new anti-*Giardia* drugs and drug targets. Ionic channels are pore-forming proteins that allow the passage of specific ions across the membrane, regulating different physiological processes (Subramanyam & Colecraft 2015). Because of their biophysical behavior and participation in different human pathologies, ionic channels are attractive targets for drug design (Bagal et al. 2013). Potassium channels are the most diverse and ubiquitous group of ion channels. They are divided into four main families on the basis of their biophysical and structural properties: voltage-gated K^+ channels, calcium-activated K^+ channels (K_{Ca}), inward-rectifier K^+ channels and two-pore-domain K^+ channels (K_{2P}) (Wulff et al. 2009). In both electrically excitable and non-excitable cells, potassium channels regulate multiple cellular functions including cell volume, proliferation, differentiation, and motility (Grunnet et al. 2002; Pchelintseva & Djamgoz 2018; Schwab et al. 2008; Urrego et al. 2014).

Recently, several studies have reported identification and characterization of K^+ channels in pathogenic protozoa. In *Plasmodium falciparum* and *Trypanosoma cruzi*, these channels are expressed in different stages of the parasite life cycle. They are essential for growth and play a significant role in parasite response to environmental stresses (Ellekvist et al. 2004; Jimenez & Docampo 2012; Waller et al. 2008). A heterodimeric Ca^{2+}-activated potassium channel was identified in *Trypanosoma brucei*. This identification was accomplished by profile searches of the predicted parasite proteome against the conserved loop of cation channels. The channel identified was found to be essential for the bloodstream form parasites (Steinmann et al. 2015). The National Center for Advancing Translational Sciences Small Molecule Repository was screened. In this screening, fluticasone propionate was identified as a potential good inhibitor of *T. brucei* potassium channels. Experiments confirmed fluticasone propionate

as a candidate drug targeting *T. brucei* (IC50 of 0.6 μM) (Schmidt et al. 2018). Biaguini and coworkers showed that K^+ causes an important depolarization of the membrane in *Giardia lamblia* (Biagini et al. 2000). Results of others studies, report that K^+ plays an important role as an osmolyte regulating *Giardia* cell volume (Maroulis et al. 2000). *Xenopus* oocytes were injected with mRNA isolated from trophozoites of *G. lamblia*, subsequent electrophysiology experiments revealed potassium currents (Ponce et al. 2013). By genome analysis and a bioinformatic approach, Prole and Marrion identified a putative potassium channel in *Giardia lamblia* assemblage *E* (Prole & Marrion 2012). However, the structural characterization of ionic channels in this protozoan is limited. Consequently, the potential of these channels to serve as a drug targets is poorly understood.

In recent years, *in silico* strategies have been used frequently to estimate protein function, for the discovery of new target molecules and for structure-based drug design studies (Chen & Chen 2008). This work describes computational approaches to determine structural biology of a putative *Giardia* potassium channel, GiK. Further, this work evaluates the potential of this channel to serve as a novel target. . A closed-state pore domain of GiK homology model was constructed. This construction was accomplished using a high conductance calcium-activated potassium channel from *Aplysia californica* (PDB ID: 5TJI) as a template. Our docking and virtual screening approach identified one hundred ten potassium channel blockers exhibiting high free energy of binding to GiK, thirty-nine of these drugs bind in the pore region of the channel. The drugs interact mainly with sites in three specific regions: S5, S2-S4 and C-terminal. These findings support the conclusion that this protein is an attractive target for biological testing to reveal its role in the life cycle of *Giardia lamblia* and a potential candidate for the design of novel antigiardial drugs.

2. Materials and Methods

2.1 *In silico* putative potassium channel identification in *Giardia*

To identify homologous sequences in *Giardia lamblia*, fifty-one potassium channel sequences from genomes of different species, deposited in the NCBI protein database (http://www.ncbi.nlm.nih.gov/protein), were compared by BLAST algorithm with the *Giardia* genome database (http://giardiadb.org/giardiadb/).

The amino acid composition, physicochemical properties, solvation and protein binding sites of the resulting sequence (GiK) (Accession number XP_001709490) were analyzed using PROTPARAM ((http://expasy.org/tools/) and PredictProtein (Yachdav et al. 2014). We applied PONDR (Predictor of Natural Disordered Regions) (Obradovic et al. 2003) to predict disorder regions. Highly conserved residues were identified by consensus results of NCBI Conserved domains (Marchler-Bauer et al. 2017), Motif Search (http://www.genome.jp/tools/motif/), InterProScan tool (Jones et al. 2014), Block Searcher (Henikoff & Henikoff 1994), and ExPASy PROSITE (Sigrist et al. 2013). Consensus results of the Constrained Consensus TOPology prediction server (Tusnady & Simon 1998; Tusnady & Simon 2001) and PredictProtein (Yachdav et al. 2014) servers were used for the prediction of transmembrane domains.

2.2 Prediction of the potassium blockers binding sites on GiK

2.2.1 Homology model and refinement

The crystal structure of GiK is not available. Therefore, three-dimensional (3D) models of the pore region (1-500 aa) were produced using I-TASSER (Iterative Threading ASSEmbly Refinement) (Roy et al. 2010; Yang et al. 2015; Zhang 2008), RaptorX (Ma et al. 2012; Ma et al. 2013; Peng & Xu 2010), Phyre2 (Protein Homology/analogY Recognition Engine V 2.0) (Kelley et al. 2015), SWISS- MODEL (Arnold et al. 2006; Biasini et al. 2014; Bordoli et al. 2008), and Modeller 9.18 (Fiser et al. 2000; Martí-Renom et al. 2000; Šali & Blundell 1993; Webb & Sali 2002). First, we searched the PDB (Berman et al. 2007) for known protein structures using the GiK sequence as query. We also searched for suitable templates in the SWISS-MODEL Template library. Next, a multiple alignment of the GiK sequence (UniProtKB accession: A8B451) to the main template structures was calculated, by MultAlin software (Corpet 1988). Optimization of the hydrogen bonding network and the atomic level energy minimization

of the 3D-GiK models generated were performed using the What If Web Interface (Chinea et al. 1995) and the 3D Refine protein structure refinement server (Bhattacharya & Cheng 2013; Bhattacharya et al. 2016). The global structural quality of predicted models was validated by RAMPAGE (Ramachandran Plot Analysis) (Lovell et al. 2003), QMEAN (Qualitative Model Energy Analysis) (Benkert et al. 2008), Verify 3D (Bowie et al. 1991; Luthy et al. 1992), ERRAT (Colovos & Yeates 1993) and ProSA-web (Wiederstein & Sippl 2007). The 3D-GiK model with the best scoring was selected for refinement using UCSF CHIMERA v1.11.1 (Pettersen et al. 2004). We used 100 steps of conjugate gradient minimization. The QMEANBrane tool was used to assess the local quality of the 3D-GiK membrane protein model (Studer et al. 2014). To confirm the quality of the models, we compare the 13 resulting 3D models with the corresponding experimental structure using the root mean square deviation (RMSD). TM-align was used to determinated the backbone Cα coordinates of the given protein structures. The results of the predicted models with Cα-RMSD are expressed in Å. The monomer was built by alignment with template 5TJI. Tetrameric assemblage was obtained by the Maestro 2017-1 software with four holo forms monomers of 5TJIs, avoiding overlapping of monomers. (Schrödinger 2017).

2.3 Molecular docking evaluation

Numerous structures of potassium blockers have been reported. To identify potential drug binding sites on the GiK protein, we selected 290 potassium blockers from the Drug bank (www.drugbank.ca), Sigma profile (www.sigmaaldrich.com) and Zinc (http://zinc.docking.org) (Irwin et al. 2012) databases. Prior to docking, all structures were energy minimized using Maestro 2017-1 (Schrödinger 2017).

The docking simulations were carried out using AutoDock Vina software, employing a Lamarckian genetic algorithm (Trott & Olson 2010), with a grid box of 126 $Å^3$ and 9 binding modes. The complexes and poses between 3D-GiK and potassium blockers were analyzed using Maestro 2017-1 (Schrödinger 2017). The results are reported as binding energy of ligand and protein in kcal/mol.

168

169 **3. Results**

170

171 **3.1 Identification and characterization of the putative potassium channel GiK**

172 We performed BLAST searches of the *Giardia* genome database. We used the whole
173 sequence of fifty-one potassium channels genomic sequences of different species as
174 queries (Supplementary Table 1). The uncharacterized protein GL50803_101194, GiK
175 (GenBank Accession: XP_001709490), showed 24-50% identity and 50-90% positivity
176 with 21 different types of voltage-gated potassium channels (Table 1). Physicochemical
177 properties were obtained (Table 2). These properties enabled establishment of GiK
178 molecular weight, stability index, isoelectric point, aliphatic index, and Grand Average of
179 Hydropathicity (GRAVY) of GiK. The instability index indicates that GiK might be
180 unstable in nature (instability index >40). The aliphatic index, a factor in protein thermal
181 stability, is related to the mole fraction of Ala, Ile, Leu, and Val in the protein. The
182 aliphatic index of GiK 93.28 indicates a thermally stable protein that contains high
183 amount of hydrophobic amino acids (Supplementary Figure 1). The negative value of
184 GRAVY indicates that GiK is a hydrophilic protein (Wilkins et al. 1999). The prediction of
185 disordered regions in GiK suggests that this protein has 11 intrinsically disordered
186 regions that could be involved in important *Giardia* functions (Supplementary Figure 2).
187 The membrane topology and the analysis of the main features of K^+ channels show that
188 GiK is a membrane protein that possesses seven helical transmembrane (HTM)
189 regions. Further, evidence shows a highly conserved pore-loop sequence that
190 determines K^+ channel selectivity (Fig. 1). According to databases of protein signatures,
191 GiK contains: a domain related to ionic channels, Ion_trans_2 domain; domains related
192 to voltage-gated potassium channels, 215625 and 236711; one domain associated with
193 signal transduction, 227696; two fingerprints of potassium channel, 2POREKCHANEL
194 and KCHANNEL; and one fingerprint related with EAG/ELK/ERG channels
195 (EAGCHANLFMLY). These results suggest that this protein is a potassium channel
196 (Fig. 2 and Table 3).

The pore-forming domain is highly conserved in all types of K^+ channels. An alignment revealed that all sequences that showed homology with GiK present the pore signature sequence S/TXGXGX. GiK has the residues SIASIGYGD, similar to TFLSIGYG, which are present in small conductance calcium-activated potassium channels (SKCa) (Shin et al. 2005) (Fig. 3). Finally, using PredictProtein server (Yachdav et al. 2014), we predicted GiK has potassium channel activity with 36% reliability.

3.2 Modeling and structure quality of GiK protein

The prediction of the 3D-GiK structure was done by homology modeling. The search for a structural template for GiK protein revealed identity with four resolved protein structures. Two structures were the open and closed state of a high conductance calcium-activated potassium channel from *Aplysia californica* (PDB ID: 5TJ6, open state, and 5TJI, closed state), with 23% sequence identity. The other two structures were the open and closed state of a potassium channel subfamily T member 1 from *Gallus gallus* (PDB: 5U70, open state, and 5U76, closed state) with 19% sequence identity (Supplementary Fig. 3).

Model construction was performed using five homology modelling servers: I-TASSER, RaptorX, Phyre2, Swiss model, and Modeller 9.18. Using the four templates, a modelling protocol was constructed for each program. The final dataset includes thirteen 3D-GiK models covering a wide range of quality. The global quality of each theoretical model was validated by the Ramachandran plot analysis, QMEAN score, Z score, ERRATscore, and Verify 3D. Modeller 9.18 program produced the best 3D-GiK model, using the sequence 5TJI as template (Table 4). Figures 4A-C show the resulting ratio of Z-score and the QMEAN score obtained for GiK. The z-score value, -5.07, is in the range of native conformations. This can be seen clearly when the score is compared to the scores of other experimentally determined protein structures with the same number of residues. Further, the QMEAN4 score is in the range of a good experimental structure (0.296). Additionally, the Ramachandran plot analysis confirms that this model is characterized by stereochemical parameters of a stable structure, with 94.2% of residues in the most favored region, 4.6% in the allowed region, and 1.2% in the disallowed region (Fig. 4). Finally, according to the QMEANBrane tool estimation, the

3D-GiK model is in the range expected for a membrane protein (Fig. 5). Figure 6 shows the monomeric and tetrameric form, and the pore cavity.

3.3 Molecular docking

Molecular docking permits prediction of the most probable position, orientation, and conformation of interactions between a ligand and macromolecule (Ferreira et al. 2015). To predict binding free energy to GiK, 290 potassium blockers were investigated (Supplementary Table 2). The overall docking energy of a given ligand molecule was expressed in kcal/mol. This approach revealed 110 molecules exhibiting the best binding free energies (-4 to -11 kcal/mol) (Table 5). Of these, 39 are commercially available compounds. Interestingly, these drugs bind in three specific hydrophobic pockets of GiK. We labeled these regions I, II, and III (Fig. 7). As shown in Table 6, 13 residues are important for binding in region I, located on the S6 transmembrane region of the channel. Of these, 10 are hydrophobic and three are polar. For region II, nine residues located on the S5-S6 linker and S6 portion of the channel interact with the various docked ligands. Of these, five are hydrophobic and four are polar. For region III, 12 extracellular residues are important for ligand interaction. Eight are hydrophobic and four are polar. The major residues observed to interact with more of the ligands were Leu65, Gly113, Gln116, Leu117, Tyr120, Met122, Phe125, Ile127 and Arg129, in region II. More negative free binding energy results in the formation of stronger complexes. We analyzed the interaction maps of the three molecules with highest binding free energies that bind to different pockets of the GiK protein. The ligand with the highest score was the K^+ channel blocker 6,10-diaza-3(1,3)8,(1,4)-dibenzena-1,5(1,4)-diquinolinacy clodecaphane (UCL 1684, -11.2 kcal/mol). This drug was observed to interact with GiK in region I forming hydrophobic interactions with Phe218, Val221, Val222, Leu225, Tyr226, Val247, Leu250 and Leu276. The competitive antagonist of $GABA_A$ receptors, bicuculline, had the highest score (-11.2 kcal/mol) for interaction with GiK in region II. This drug forms: hydrophobic interactions with Gly113, Gln116, Leu117, Tyr118, Tyr120, Met122, Ser124, Phe125, Ser126 and Arg129. Further, bicuculline forms π-π interactions with Phe125 and Tyr68. Finally, the bioactive alkaloid, verruculogen, interacts with GiK site III by hydrophobic interactions with Val348, Pro347, Val377,

Met378 and Ile411. Further, verruculogen interacts by polar interaction with Ser346 (Table 6, Fig. 8).

4. Discussion

In this report, we provide *in silico* evidence indicating the protein XP_001709490 from *Giardia lamblia* (GiK) is a membrane protein, with conserved potassium channels features. GiK presents seven HTM regions and the pore signature sequence SIASIGYGD. This sequence is associated with K^+ selectivity in small conductance calcium-activated potassium channels. The presence of the Ion_trans_2 domain related to voltage-gated potassium channels suggests that GiK could be activated by either electrical means or by increasing calcium concentrations in the cell. Additional studies are necessary to understand the voltage-gated and ion selectivity in GiK.

Transmembrane protein GiK presents hydrophobic regions containing a high fraction of non-polar amino acids. It also presents hydrophilic regions containing a high fraction of polar amino acids (Supplementary Figures 1 and 4). The GRAVY value of -0.053 indicates that GiK could establish interactions with water; it can be highly hydrated in aqueous media. GiK contains protein regions that do not fold into defined tertiary structure. These are structural disorders commonly labeled intrinsically disordered regions (IDRs). IDRs perform a central role in regulation of signaling pathways and crucial cellular processes. They are frequently associated with disease. For these reasons, there is growing interest in IDRs as potential targets for drug design (Calcada et al. 2015; Cheng et al. 2006). The prediction of 14 flexible disordered regions in GiK suggests that this protein may be important in various *Giardia* functions. This important preliminary evidence indicates that GiK is a promising subject for future study.

Potassium channels regulate multiple cellular functions in both electrically excitable and non-excitable cells. Therefore, they are attractive targets for drug design. Current trends in drug discovery focus on target identification and *in silico* compound design. We sought to determine whether GiK could be a potential drug target in *Giardia*. First, we built structural models of the transmembrane helical regions of GiK by homology

modeling. The search for templates showed only two resolved structures: a high conductance calcium-activated potassium channel from *Aplysia californica* (PDB ID: 5TJ6 and 5TJI) and a potassium channel subfamily T member 1 from *Gallus gallus* (PDB: 5U70 and 5U76). In this work, GiK presents 23 and 19% of sequence identity with the templates. Root Mean Square Deviation (RMSD) is a quantitative measure of the similarity between two superimposed atomic coordinates. When using RMSD to compare protein structures, the RMSD distribution depends on the size of the protein and of the homology between the templates, among others (Kufareva & Abagyan 2012). Using multiple approaches we generated 13 structural models of GiK, the quality analysis of individual models showed that even though, models obtained with Swiss model and Phyre2 had the lower RMSD values, only 50-70% of residues were modelled. The percentage of residues in the allowed regions was expected to be more than 90% for a good model. The Modeller program produced acceptable models. The best result was obtained employing the PDB ID: 5TJI (closed state); 500 a.a aligned, results from a Ramachandran plot showed 94.2% of residues in the most favored region. Even though the structures obtained with 5U70 and 5TJ6 showed 90% of residues in the most favored region, the overall quality factor (Bagal et al.) value of 5TJI is the highest (69.24%) and is within the accepted range. Besides, it is important to emphasize that in addition to RMSD, the generation of Z-score is also a measure of statistical significance between matched structures and reflects the degree of modelling success (Dalton & Jackson 2007), the *Z*-score value (-5.07) indicates that the overall geometrical quality of the model generated by Modeller using the template 5TJI was within the acceptable range for big proteins. The overall results from RAMPAGE, QMEAN and Verify 3D indicate the 3D modeled GiK protein is of good quality. After building the 3D structure of GiK, we screened 290 potassium channel blockers. The docking results showed 110 potassium channel blockers with high affinity for the GiK protein. Thirty-nine of these showed similar binding modes in three specific regions, labelled I to III. They interact principally with hydrophobic and aromatic residues such as Phe, Tyr, Leu and Val. In agreement with results described for different potassium blockers, the ring stacking, hydrophobic interactions with several aromatic side chains and polar interactions take place mainly in S5 and S6 (Marzian et al. 2013; Saxena et

al. 2016). The ionic channels can be switched or gated between an open and closed state by external signals such as changes in transmembrane voltage, binding of ligands, and mechanical stress. Some K^+ channels possess a highly hydrophobic inner pore that can function as an effective barrier to ion permeation (Aryal et al. 2015). Our results suggest that GiK is a calcium potassium activated channel with a hydrophobic inner pore. Additional research is needed to confirm this finding. We plan to expand our studies in this area in the future. (Liu & Kokubo 2017; Martins et al. 2018).

Other authors have reported successful computational screening of K^+ channels. These reports demonstrate that computational screening is an effective method for rapidly discovering new channels blockers from large databases (Kingsley et al. 2017; Liu et al. 2003). Hong Liu and coworkers identified 14 natural compound of relatively lower binding energy. These researchers used a docking virtual screening approach based upon a three-dimensional model of the eukaryotic K^+ channels. Experimental results showed that four of these exerted potent and selective inhibitory effect on K^+ channels (Liu et al. 2003). Interestingly, some of the potassium channel blockers in our study have been employed with some success for their antiparasite activity. Verruculogen, clofilium, clotrimazole, trifluoroperazine, bicuculline methiodide, tubocurarin, and dequalinium chloride affect the growth of *Trypanosoma bruceii*, *Leishmania donovani, Plasmodium falciparum and Trichomonas vaginalis* (Della Casa et al. 2002; Nam et al. 2011; Rateb et al. 2013; Waller et al. 2008). Quinidine inhibits the cell division in *Tetrahymena pyriformis* (Conklin et al. 1970). Trifluoperazine alters the motility in *Paramecium sp.* (Otter et al. 1984). Disodium cromoglycate and terfenadine show activity in infection models of *Toxoplasma gondii* and *Plasmodium yoelli nigeriensis* (Rezaei et al. 2016; Singh & Puri 1998). In *Giardia lamblia*, trifluoroperazine, a calmodulin antagonist, inhibits excystment (Bernal et al. 1998). It remains uncertain whether potassium channels are the targets of these compounds.

5. Conclusion

Using structural bioinformatics, we identified the hypothetical protein XP_001709490 from *Giardia lamblia* as a potassium channel, GiK. By protein docking analysis, we found 39 commercial potassium channel blockers that have affinity for this protein.

These blockers are predicted to bind in three specific regions on the protein. The novelty of this work lies in the use of the model 3D-GiK structure to screen compounds with theoretical affinity. Some of the drugs predicted by the model to be effective have demonstrated antiparasitic activity in *in vitro* and *in vivo* assays. Experimental analyses are needed to confirm the activity of these drugs on *Giardia*. The low homology of GiK with proteins in the human genome contributes to its potential as a target of specific pharmacological agents.

6. References

Ansell BR, McConville MJ, Ma'ayeh SY, Dagley MJ, Gasser RB, Svard SG, and Jex AR. 2015. Drug resistance in Giardia duodenalis. *Biotechnol Adv* 33:888-901. 10.1016/j.biotechadv.2015.04.009

Arnold K, Bordoli L, Kopp J, and Schwede T. 2006. The SWISS-MODEL workspace: a web-based environment for protein structure homology modelling. *Bioinformatics* 22:195-201. 10.1093/bioinformatics/bti770

Aryal P, Sansom MS, and Tucker SJ. 2015. Hydrophobic gating in ion channels. *J Mol Biol* 427:121-130. 10.1016/j.jmb.2014.07.030

Bagal SK, Brown AD, Cox PJ, Omoto K, Owen RM, Pryde DC, Sidders B, Skerratt SE, Stevens EB, Storer RI, and Swain NA. 2013. Ion channels as therapeutic targets: a drug discovery perspective. *J Med Chem* 56:593-624. 10.1021/jm3011433

Benkert P, Tosatto SCE, and Schomburg D. 2008. QMEAN: A comprehensive scoring function for model quality assessment. *Proteins: Structure, Function, and Bioinformatics* 71:261-277. 10.1002/prot.21715

Berman H, Henrick K, Nakamura H, and Markley JL. 2007. The worldwide Protein Data Bank (wwPDB): ensuring a single, uniform archive of PDB data. *Nucleic Acids Res* 35:D301-303. 10.1093/nar/gkl971

Bernal RM, Tovar R, Santos JI, and Munoz ML. 1998. Possible role of calmodulin in excystation of Giardia lamblia. *Parasitol Res* 84:687-693.

Bhattacharya D, and Cheng J. 2013. 3Drefine: Consistent protein structure refinement by optimizing hydrogen bonding network and atomic-level energy minimization. *Proteins: Structure, Function, and Bioinformatics* 81:119-131. 10.1002/prot.24167

Bhattacharya D, Nowotny J, Cao R, and Cheng J. 2016. 3Drefine: an interactive web server for efficient protein structure refinement. *Nucleic Acids Research* 44:W406-W409. 10.1093/nar/gkw336

Biagini GA, Lloyd D, Kirk K, and Edwards MR. 2000. The membrane potential of Giardia intestinalis. *FEMS Microbiol Lett* 192:153-157.

Biasini M, Bienert S, Waterhouse A, Arnold K, Studer G, Schmidt T, Kiefer F, Cassarino TG, Bertoni M, Bordoli L, and Schwede T. 2014. SWISS-MODEL: modelling protein tertiary and quaternary structure using evolutionary information. *Nucleic Acids Research* 42:W252-W258. 10.1093/nar/gku340

388 Bordoli L, Kiefer F, Arnold K, Benkert P, Battey J, and Schwede T. 2008. Protein structure
389 homology modeling using SWISS-MODEL workspace. *Nat Protocols* 4:1-13.
390 Bowie J, Luthy R, and Eisenberg D. 1991. A method to identify protein sequences that
391 fold into a known three-dimensional structure. *Science* 253:164-170.
392 10.1126/science.1853201
393 Calcada EO, Korsak M, and Kozyreva T. 2015. Recombinant Intrinsically Disordered
394 Proteins for NMR: Tips and Tricks. *Adv Exp Med Biol* 870:187-213. 10.1007/978-
395 3-319-20164-1_6
396 Carter ER, Nabarro LE, Hedley L, and Chiodini PL. 2018. Nitroimidazole-refractory
397 giardiasis: a growing problem requiring rational solutions. *Clin Microbiol Infect*
398 24:37-42. 10.1016/j.cmi.2017.05.028
399 Colovos C, and Yeates TO. 1993. Verification of protein structures: patterns of
400 nonbonded atomic interactions. *Protein Science : A Publication of the Protein*
401 *Society* 2:1511-1519.
402 Conklin KA, Heu P, and Chou SC. 1970. Quinine--effect on Tetrahymena pyriformis. II.
403 Comparative activity of the stereoisomers, quinidine and quinine. *J Pharm Sci*
404 59:704-705.
405 Corpet F. 1988. Multiple sequence alignment with hierarchical clustering. *Nucleic Acids*
406 *Res* 16:10881-10890.
407 Chen YP, and Chen F. 2008. Identifying targets for drug discovery using bioinformatics.
408 *Expert Opin Ther Targets* 12:383-389. 10.1517/14728222.12.4.383
409 Cheng Y, LeGall T, Oldfield CJ, Mueller JP, Van YY, Romero P, Cortese MS, Uversky
410 VN, and Dunker AK. 2006. Rational drug design via intrinsically disordered protein.
411 *Trends Biotechnol* 24:435-442. 10.1016/j.tibtech.2006.07.005
412 Chinea G, Padron G, Hooft RWW, Sander C, and Vriend G. 1995. The use of position-
413 specific rotamers in model building by homology. *Proteins: Structure, Function,*
414 *and Bioinformatics* 23:415-421. 10.1002/prot.340230315
415 Dalton JA, and Jackson RM. 2007. An evaluation of automated homology modelling
416 methods at low target template sequence similarity. *Bioinformatics* 23:1901-1908.
417 10.1093/bioinformatics/btm262
418 Della Casa V, Noll H, Gonser S, Grob P, Graf F, and Pohlig G. 2002. Antimicrobial activity
419 of dequalinium chloride against leading germs of vaginal infections.
420 *Arzneimittelforschung* 52:699-705. 10.1055/s-0031-1299954
421 Ellekvist P, Ricke CH, Litman T, Salanti A, Colding H, Zeuthen T, and Klaerke DA. 2004.
422 Molecular cloning of a K(+) channel from the malaria parasite Plasmodium
423 falciparum. *Biochem Biophys Res Commun* 318:477-484.
424 10.1016/j.bbrc.2004.04.049
425 Escobedo AA, and Cimerman S. 2007. Giardiasis: a pharmacotherapy review. *Expert*
426 *Opin Pharmacother* 8:1885-1902. 10.1517/14656566.8.12.1885
427 Ferreira LG, Dos Santos RN, Oliva G, and Andricopulo AD. 2015. Molecular docking and
428 structure-based drug design strategies. *Molecules* 20:13384-13421.
429 10.3390/molecules200713384
430 Fiser A, Do RK, and Sali A. 2000. Modeling of loops in protein structures. *Protein Science*
431 *: A Publication of the Protein Society* 9:1753-1773.

Grunnet M, MacAulay N, Jorgensen NK, Jensen B, Olesen S-P, and Klaerke DA. 2002. Regulation of cloned, Ca2+-activated K+ channels by cell volume changes. *Pflügers Archiv* 444:167-177. 10.1007/s00424-002-0782-4

Henikoff S, and Henikoff JG. 1994. Protein family classification based on searching a database of blocks. *Genomics* 19:97-107. 10.1006/geno.1994.1018

Irwin JJ, Sterling T, Mysinger MM, Bolstad ES, and Coleman RG. 2012. ZINC: a free tool to discover chemistry for biology. *J Chem Inf Model* 52:1757-1768. 10.1021/ci3001277

Jimenez V, and Docampo R. 2012. Molecular and electrophysiological characterization of a novel cation channel of Trypanosoma cruzi. *PLoS Pathog* 8:e1002750. 10.1371/journal.ppat.1002750

Jones P, Binns D, Chang HY, Fraser M, Li W, McAnulla C, McWilliam H, Maslen J, Mitchell A, Nuka G, Pesseat S, Quinn AF, Sangrador-Vegas A, Scheremetjew M, Yong SY, Lopez R, and Hunter S. 2014. InterProScan 5: genome-scale protein function classification. *Bioinformatics* 30:1236-1240. 10.1093/bioinformatics/btu031

Kelley LA, Mezulis S, Yates CM, Wass MN, and Sternberg MJE. 2015. The Phyre2 web portal for protein modeling, prediction and analysis. *Nat Protocols* 10:845-858. 10.1038/nprot.2015.053

Kingsley B, Kumari S, Appian S, and Brindha P. 2017. *In silico Docking Studies on ATP-Sensitive K+Channel, Insulin Receptor and Phosphorylase kinase Activity by Isolated Active Principles of Stereospermum tetragonum DC*.

Kufareva I, and Abagyan R. 2012. Methods of protein structure comparison. *Methods Mol Biol* 857:231-257. 10.1007/978-1-61779-588-6_10

Leitsch D. 2015. Drug Resistance in the Microaerophilic Parasite Giardia lamblia. *Curr Trop Med Rep* 2:128-135. 10.1007/s40475-015-0051-1

Liu H, Li Y, Song M, Tan X, Cheng F, Zheng S, Shen J, Luo X, Ji R, Yue J, Hu G, Jiang H, and Chen K. 2003. Structure-based discovery of potassium channel blockers from natural products: virtual screening and electrophysiological assay testing. *Chem Biol* 10:1103-1113.

Liu K, and Kokubo H. 2017. Exploring the Stability of Ligand Binding Modes to Proteins by Molecular Dynamics Simulations: A Cross-docking Study. *J Chem Inf Model* 57:2514-2522. 10.1021/acs.jcim.7b00412

Lovell SC, Davis IW, Arendall WB, de Bakker PIW, Word JM, Prisant MG, Richardson JS, and Richardson DC. 2003. Structure validation by Cα geometry: ϕ,ψ and Cβ deviation. *Proteins: Structure, Function, and Bioinformatics* 50:437-450. 10.1002/prot.10286

Luthy R, Bowie JU, and Eisenberg D. 1992. Assessment of protein models with three-dimensional profiles. *Nature* 356:83-85.

Ma J, Peng J, Wang S, and Xu J. 2012. A conditional neural fields model for protein threading. *Bioinformatics* 28:i59-i66. 10.1093/bioinformatics/bts213

Ma J, Wang S, Zhao F, and Xu J. 2013. Protein threading using context-specific alignment potential. *Bioinformatics* 29:i257-i265. 10.1093/bioinformatics/btt210

Marchler-Bauer A, Bo Y, Han L, He J, Lanczycki CJ, Lu S, Chitsaz F, Derbyshire MK, Geer RC, Gonzales NR, Gwadz M, Hurwitz DI, Lu F, Marchler GH, Song JS, Thanki N, Wang Z, Yamashita RA, Zhang D, Zheng C, Geer LY, and Bryant SH.

2017. CDD/SPARCLE: functional classification of proteins via subfamily domain architectures. *Nucleic Acids Res* 45:D200-D203. 10.1093/nar/gkw1129

Maroulis SL, Schofield PJ, and Edwards MR. 2000. The role of potassium in the response of Giardia intestinalis to hypo-osmotic stress. *Mol Biochem Parasitol* 108:141-145.

Martí-Renom MA, Stuart AC, Fiser A, Sánchez R, and FM, and Šali A. 2000. Comparative Protein Structure Modeling of Genes and Genomes. *Annual Review of Biophysics and Biomolecular Structure* 29:291-325. 10.1146/annurev.biophys.29.1.291

Martins LC, Torres PHM, de Oliveira RB, Pascutti PG, Cino EA, and Ferreira RS. 2018. Investigation of the binding mode of a novel cruzain inhibitor by docking, molecular dynamics, ab initio and MM/PBSA calculations. *J Comput Aided Mol Des* 32:591-605. 10.1007/s10822-018-0112-3

Marzian S, Stansfeld PJ, Rapedius M, Rinne S, Nematian-Ardestani E, Abbruzzese JL, Steinmeyer K, Sansom MS, Sanguinetti MC, Baukrowitz T, and Decher N. 2013. Side pockets provide the basis for a new mechanism of Kv channel-specific inhibition. *Nat Chem Biol* 9:507-513. 10.1038/nchembio.1271

Nam TG, McNamara CW, Bopp S, Dharia NV, Meister S, Bonamy GM, Plouffe DM, Kato N, McCormack S, Bursulaya B, Ke H, Vaidya AB, Schultz PG, and Winzeler EA. 2011. A chemical genomic analysis of decoquinate, a Plasmodium falciparum cytochrome b inhibitor. *ACS Chem Biol* 6:1214-1222. 10.1021/cb200105d

Obradovic Z, Peng K, Vucetic S, Radivojac P, Brown CJ, and Dunker AK. 2003. Predicting intrinsic disorder from amino acid sequence. *Proteins* 53 Suppl 6:566-572. 10.1002/prot.10532

Otter T, Satir BH, and Satir P. 1984. Trifluoperazine-induced changes in swimming behavior of paramecium: evidence for two sites of drug action. *Cell Motil* 4:249-267.

Pchelintseva E, and Djamgoz MBA. 2018. Mesenchymal stem cell differentiation: Control by calcium-activated potassium channels. *J Cell Physiol* 233:3755-3768. 10.1002/jcp.26120

Peng J, and Xu J. 2010. Low-homology protein threading. *Bioinformatics* 26:i294-300. 10.1093/bioinformatics/btq192

Pettersen EF, Goddard TD, Huang CC, Couch GS, Greenblatt DM, Meng EC, and Ferrin TE. 2004. UCSF Chimera--a visualization system for exploratory research and analysis. *J Comput Chem* 25:1605-1612. 10.1002/jcc.20084

Ponce A, Jimenez-Cardoso E, and Eligio-Garcia L. 2013. Voltage-dependent potassium currents expressed in Xenopus laevis oocytes after injection of mRNA isolated from trophozoites of Giardia lamblia (strain Portland-1). *Physiol Rep* 1:e00186. 10.1002/phy2.186

Prole DL, and Marrion NV. 2012. Identification of putative potassium channel homologues in pathogenic protozoa. *PloS one* 7:e32264.

Rateb ME, Hallyburton I, Houssen WE, Bull AT, Goodfellow M, Santhanam R, Jaspars M, and Ebel R. 2013. Induction of diverse secondary metabolites in Aspergillus fumigatus by microbial co-culture. *RSC Advances* 3:14444. 10.1039/c3ra42378f

Rezaei F, Ebrahimzadeh MA, Daryani A, Sharif M, Ahmadpour E, and Sarvi S. 2016. The inhibitory effect of cromolyn sodium and ketotifen on Toxoplasma gondii entrance into host cells in vitro and in vivo. *J Parasit Dis* 40:1001-1005. 10.1007/s12639-014-0623-3

524 Roy A, Kucukural A, and Zhang Y. 2010. I-TASSER: a unified platform for automated
525 protein structure and function prediction. *Nature protocols* 5:725-738.
526 10.1038/nprot.2010.5
527 Šali A, and Blundell TL. 1993. Comparative Protein Modelling by Satisfaction of Spatial
528 Restraints. *J Mol Biol* 234:779-815. http://dx.doi.org/10.1006/jmbi.1993.1626
529 Saxena P, Zangerl-Plessl EM, Linder T, Windisch A, Hohaus A, Timin E, Hering S, and
530 Stary-Weinzinger A. 2016. New potential binding determinant for hERG channel
531 inhibitors. *Sci Rep* 6:24182. 10.1038/srep24182
532 Schmidt RS, Macedo JP, Steinmann ME, Salgado AG, Butikofer P, Sigel E, Rentsch D,
533 and Maser P. 2018. Transporters of Trypanosoma brucei-phylogeny, physiology,
534 pharmacology. *FEBS J* 285:1012-1023. 10.1111/febs.14302
535 Schrödinger L. 2017. Schrödinger Release 2017-1:. Maestro. New York, NY.
536 Schwab A, Hanley P, Fabian A, and Stock C. 2008. Potassium channels keep mobile
537 cells on the go. *Physiology (Bethesda)* 23:212-220. 10.1152/physiol.00003.2008
538 Shin N, Soh H, Chang S, Kim DH, and Park CS. 2005. Sodium permeability of a cloned
539 small-conductance calcium-activated potassium channel. *Biophys J* 89:3111-
540 3119. 10.1529/biophysj.105.069542
541 Sigrist CJ, de Castro E, Cerutti L, Cuche BA, Hulo N, Bridge A, Bougueleret L, and
542 Xenarios I. 2013. New and continuing developments at PROSITE. *Nucleic Acids*
543 *Res* 41:D344-347. 10.1093/nar/gks1067
544 Singh N, and Puri SK. 1998. Causal prophylactic activity of antihistaminic agents against
545 Plasmodium yoelii nigeriensis infection in Swiss mice. *Acta Trop* 69:255-260.
546 Steinmann ME, Gonzalez-Salgado A, Butikofer P, Maser P, and Sigel E. 2015. A
547 heteromeric potassium channel involved in the modulation of the plasma
548 membrane potential is essential for the survival of African trypanosomes. *FASEB*
549 *J* 29:3228-3237. 10.1096/fj.15-271353
550 Studer G, Biasini M, and Schwede T. 2014. Assessing the local structural quality of
551 transmembrane protein models using statistical potentials (QMEANBrane).
552 *Bioinformatics* 30:i505-i511. 10.1093/bioinformatics/btu457
553 Subramanyam P, and Colecraft HM. 2015. Ion channel engineering: perspectives and
554 strategies. *J Mol Biol* 427:190-204. 10.1016/j.jmb.2014.09.001
555 Tejman-Yarden N, and Eckmann L. 2011. New approaches to the treatment of giardiasis.
556 *Curr Opin Infect Dis* 24:451-456. 10.1097/QCO.0b013e32834ad401
557 Trott O, and Olson AJ. 2010. AutoDock Vina: improving the speed and accuracy of
558 docking with a new scoring function, efficient optimization, and multithreading. *J*
559 *Comput Chem* 31:455-461. 10.1002/jcc.21334
560 Tusnady GE, and Simon I. 1998. Principles governing amino acid composition of integral
561 membrane proteins: application to topology prediction. *J Mol Biol* 283:489-506.
562 10.1006/jmbi.1998.2107
563 Tusnady GE, and Simon I. 2001. The HMMTOP transmembrane topology prediction
564 server. *Bioinformatics* 17:849-850.
565 Urrego D, Tomczak AP, Zahed F, Stuhmer W, and Pardo LA. 2014. Potassium channels
566 in cell cycle and cell proliferation. *Philos Trans R Soc Lond B Biol Sci*
567 369:20130094. 10.1098/rstb.2013.0094

568 Waller KL, McBride SM, Kim K, and McDonald TV. 2008. Characterization of two putative
569 potassium channels in Plasmodium falciparum. *Malar J* 7:19. 10.1186/1475-2875-
570 7-19
571 Watkins RR, and Eckmann L. 2014. Treatment of giardiasis: current status and future
572 directions. *Curr Infect Dis Rep* 16:396. 10.1007/s11908-014-0396-y
573 Webb B, and Sali A. 2002. Comparative Protein Structure Modeling Using MODELLER.
574 *Current Protocols in Bioinformatics*: John Wiley & Sons, Inc.
575 Wiederstein M, and Sippl MJ. 2007. ProSA-web: interactive web service for the
576 recognition of errors in three-dimensional structures of proteins. *Nucleic Acids*
577 *Research* 35:W407-W410. 10.1093/nar/gkm290
578 Wilkins MR, Gasteiger E, Bairoch A, Sanchez JC, Williams KL, Appel RD, and
579 Hochstrasser DF. 1999. Protein identification and analysis tools in the ExPASy
580 server. *Methods Mol Biol* 112:531-552.
581 Wulff H, Castle NA, and Pardo LA. 2009. Voltage-gated potassium channels as
582 therapeutic targets. *Nat Rev Drug Discov* 8:982-1001. 10.1038/nrd2983
583 Yachdav G, Kloppmann E, Kajan L, Hecht M, Goldberg T, Hamp T, Honigschmid P,
584 Schafferhans A, Roos M, Bernhofer M, Richter L, Ashkenazy H, Punta M,
585 Schlessinger A, Bromberg Y, Schneider R, Vriend G, Sander C, Ben-Tal N, and
586 Rost B. 2014. PredictProtein--an open resource for online prediction of protein
587 structural and functional features. *Nucleic Acids Res* 42:W337-343.
588 10.1093/nar/gku366
589 Yang J, Yan R, Roy A, Xu D, Poisson J, and Zhang Y. 2015. The I-TASSER Suite: protein
590 structure and function prediction. *Nature methods* 12:7-8. 10.1038/nmeth.3213
591 Zhang Y. 2008. I-TASSER server for protein 3D structure prediction. *BMC Bioinformatics*
592 9:40-40. 10.1186/1471-2105-9-40

593

594

Figure 1(on next page)

Transmembrane structure of GiK.

It contains seven transmembrane segments (S1-S7), the P-loops between S5 and S6 form the pore domain. The selectivity filter is in gray.

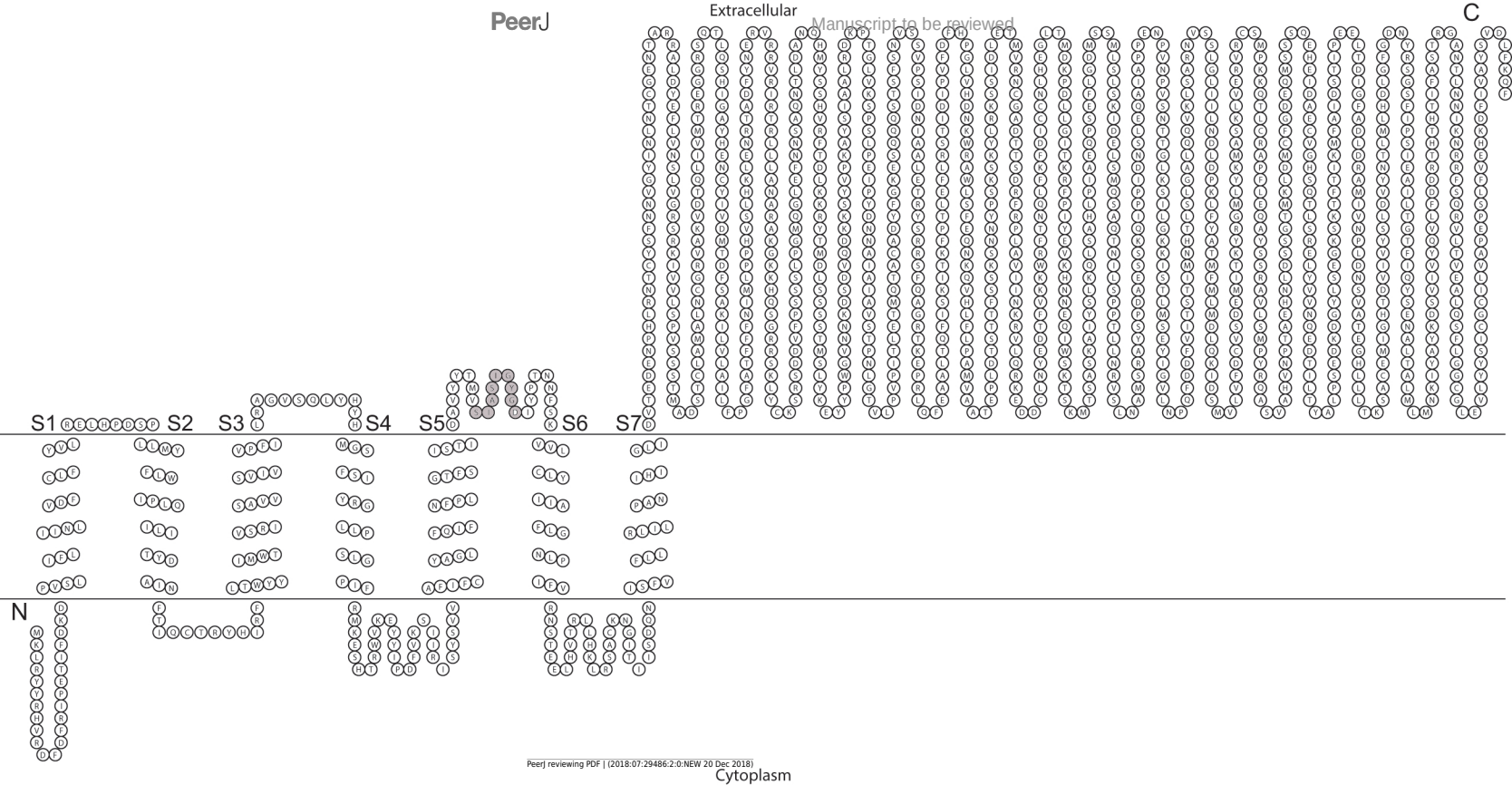
Extracellular
C
S1
S2
S3
S4
S5
S6
S7
N
Cytoplasm

Figure 2(on next page)

Domains and motifs related to potassium channels.

GiK presents domains related to different subtypes of potassium channels. **A.** Schematic representation. **B.** Accession number and description of the sequences.

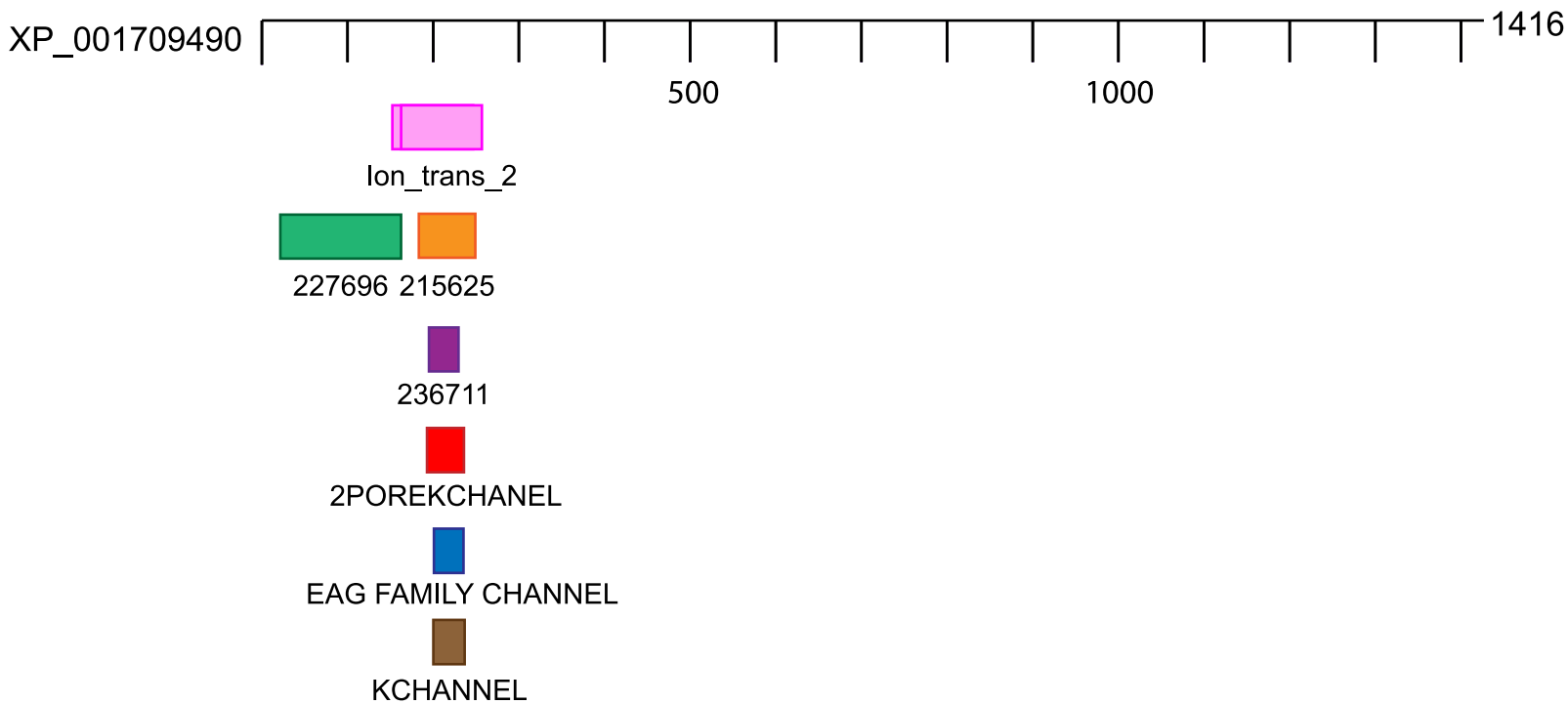

ID	Position	Sequence
pfam07885	168..245	VVAFIFCYAGLFQIFNFPLGTFSISTIDAVYYTMVSIASIGYGDIYPTNNFSKVVLCLYIIAFLG NLPIFVRNSTEEL
COG5409	12..170	FDFRIPETIFDKDPVSLIFLIINLVDFCLFYVLRELHPDSPLLMYFLWIPLQILITYDAINFTIQCT RYHIRFLTWYYIMWTVSRISAVVSVIVVPFILRAGVSQLYHYHMGSFSIYRGLLPSLGPIFRM KESHTRWVKEYYIPDFVKSIIRISYSVVA
PLN03192	181..242	IFNFPLGTFSISTIDAVYYTMVSIASIGYGDIYPTNNFSKVVLCLYIIAFLGNLPIFVRNST
PRK10537	196..214	AVYYTMVSIASIGYGDIYP
PR01333	202..230	VSIASIGYGDIYPTNNFSKVVLCLYIIAF
PR01463	193..210	TIDAVYYTMVSIASIGYG
PR00169	190..212	SISTIDAVYYTMVSIASIGYGDI

Figure 3

Multiple sequence alignment of GiK with voltage-gated potassium channels.

The signature sequence T/SXGXGX of the selectivity filter is present in all classes of potassium channels (black square).

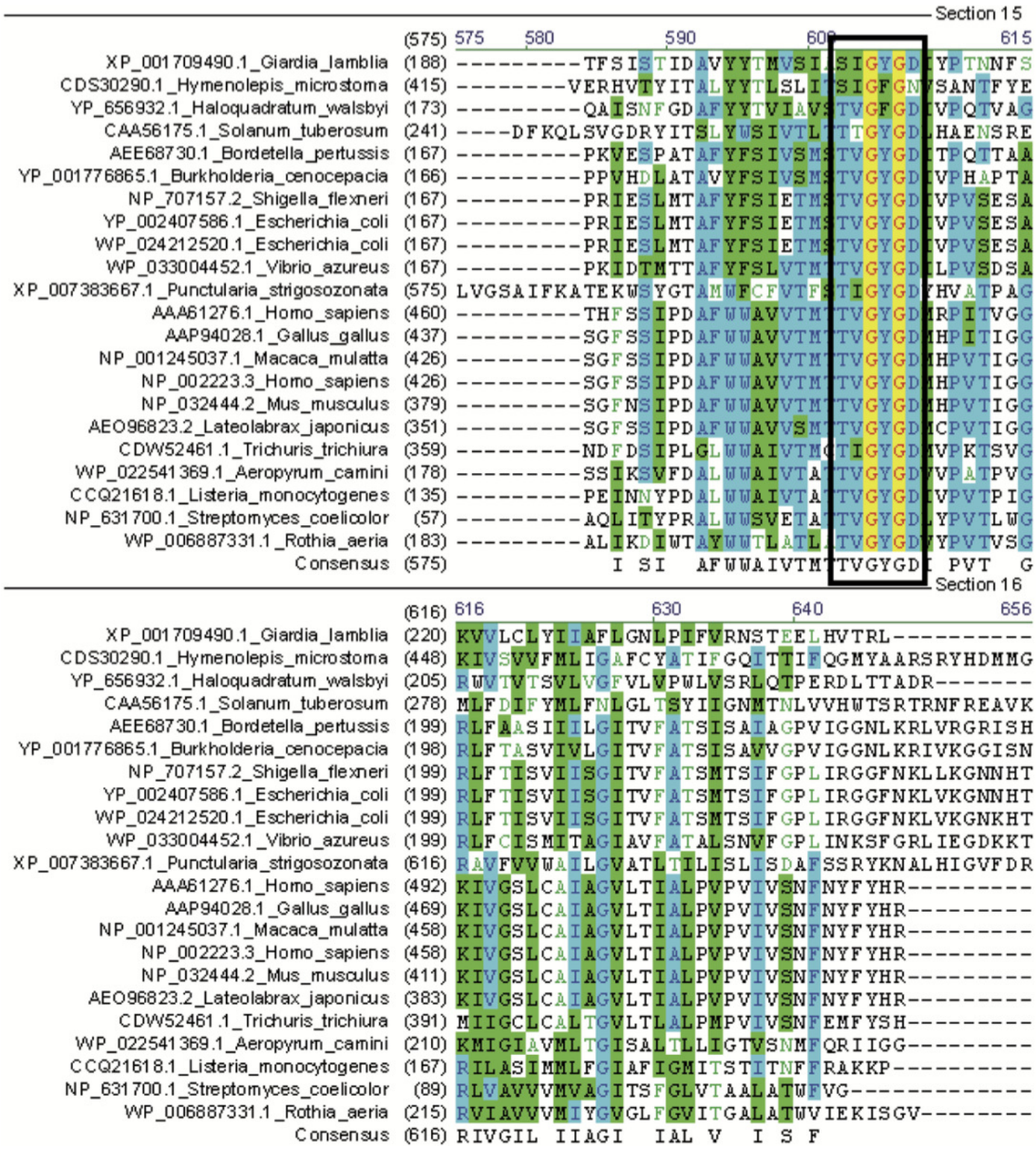
Section 15
(575) 575 580 590 600 615
XP_001709490.1_Giardia_lamblia (188) ---------TFSISTIDAVYYTMVSIASIGYGDIYPTNNFS
CDS30290.1_Hymenolepis_microstoma (415) --------VERHVTYITALYYTLSLITSIGFGNVSANTFYE
YP_656932.1_Haloquadratum_walsbyi (173) ---------QAISNFGDAFYYTVIAVSTVGFGDIVPQTVAG
CAA56175.1_Solanum_tuberosum (241) ----DFKQLSVGDRYITSLYWSIVTLTTTGYGDLHAENSRE
AEE68730.1_Bordetella_pertussis (167) ---------PKVESPATAFYFSIVSMSTVGYGDITPQTTAA
YP_001776865.1_Burkholderia_cenocepacia (166) ---------PPVHDLATAVYFSIVSMSTVGYGDIVPHAPTA
NP_707157.2_Shigella_flexneri (167) ---------PRIESLMTAFYFSIETMSTVGYGDIVPVSESA
YP_002407586.1_Escherichia_coli (167) ---------PRIESLMTAFYFSIETMSTVGYGDIVPVSESA
WP_024212520.1_Escherichia_coli (167) ---------PRIESLMTAFYFSIETMSTVGYGDIVPVSESA
WP_033004452.1_Vibrio_azureus (167) ---------PKIDTMTTAFYFSLVTMTTVGYGDILPVSDSA
XP_007383667.1_Punctularia_strigosozonata (575) LVGSAIFKATEKWSYGTAMWFCFVTFSTIGYGDYHVATPAG
AAA61276.1_Homo_sapiens (460) ---------THFSSIPDAFWWAVVTMTTVGYGDMRPITVGG
AAP94028.1_Gallus_gallus (437) ---------SGFSSIPDAFWWAVVTMTTVGYGDMHPITIGG
NP_001245037.1_Macaca_mulatta (426) ---------SGFSSIPDAFWWAVVTMTTVGYGDMHPVTIGG
NP_002223.3_Homo_sapiens (426) ---------SGFSSIPDAFWWAVVTMTTVGYGDMHPVTIGG
NP_032444.2_Mus_musculus (379) ---------SGFNSIPDAFWWAVVTMTTVGYGDMHPVTIGG
AEO96823.2_Lateolabrax_japonicus (351) ---------SGFSSIPDAFWWAVVSMTTVGYGDMCPVTIGG
CDW52461.1_Trichuris_trichiura (359) ---------NDFDSIPLGLWWAIVTMGTIGYGDMVPKTSVG
WP_022541369.1_Aeropyrum_camini (178) ---------SSIKSVFDALWWAIVTATTVGYGDYVPATPVG
CCQ21618.1_Listeria_monocytogenes (135) ---------PEINNYPDALWWAIVTATTVGYGDIVPVTPIG
NP_631700.1_Streptomyces_coelicolor (57) ---------AQLITYPRALWWSVETATTVGYGDLYPVTLWG
WP_006887331.1_Rothia_aeria (183) ---------ALIKDIWTAYWWTLATLITVGYGDVYPVTVSG
Consensus (575) I SI AFWWAIVTMTTVGYGDI PVT G
Section 16
(616) 616 630 640 656
XP_001709490.1_Giardia_lamblia (220) KVVLCLYIIAFLGNLPIFVRNSTEELHVTRL----------
CDS30290.1_Hymenolepis_microstoma (448) KIVSVVFMLIGAFCYATIFGQITTIFQGMYAARSRYHDMMG
YP_656932.1_Haloquadratum_walsbyi (205) RWVTVTSVLVGFVLVPWLVSRLQTPERDLTTADR-------
CAA56175.1_Solanum_tuberosum (278) MLFDIFYMLFNLGLTSYIIGNMTNLVVHWTSRTRNFREAVK
AEE68730.1_Bordetella_pertussis (199) RLFAASIIILGITVFATSISAIAGPVIGGNLKRLVRGRISH
YP_001776865.1_Burkholderia_cenocepacia (198) RLFTASVIVLGITVFATSISAVVGPVIGGNLKRIVKGGISN
NP_707157.2_Shigella_flexneri (199) RLFTISVIISGITVFATSMTSIFGPLIRGGFNKLLKGNNHT
YP_002407586.1_Escherichia_coli (199) RLFTISVIISGITVFATSMTSIFGPLIRGGFNKLVKGNNHT
WP_024212520.1_Escherichia_coli (199) RLFTISVIISGITVFATSMTSIFGPLIRGGFNKLVKGNKHT
WP_033004452.1_Vibrio_azureus (199) RLFCISMITAGIAVFATALSNVFGPLINKSFGRLIEGDKKT
XP_007383667.1_Punctularia_strigosozonata (616) RAVFVVWAILGVATLTILISLISDAFSSRYKNALHIGVFDR
AAA61276.1_Homo_sapiens (492) KIVGSLCAIAGVLTIALPVPVIVSNFNYFYHR---------
AAP94028.1_Gallus_gallus (469) KIVGSLCAIAGVLTIALPVPVIVSNFNYFYHR---------
NP_001245037.1_Macaca_mulatta (458) KIVGSLCAIAGVLTIALPVPVIVSNFNYFYHR---------
NP_002223.3_Homo_sapiens (458) KIVGSLCAIAGVLTIALPVPVIVSNFNYFYHR---------
NP_032444.2_Mus_musculus (411) KIVGSLCAIAGVLTIALPVPVIVSNFNYFYHR---------
AEO96823.2_Lateolabrax_japonicus (383) KIVGSLCAIAGVLTIALPVPVIVSNFNYFYHR---------
CDW52461.1_Trichuris_trichiura (391) MIIGCLCALTGVLTLALPMPVIVSNFEMFYSH---------
WP_022541369.1_Aeropyrum_camini (210) KMIGIAVMLTGISALTLLIGTVSNMFQRIIGG---------
CCQ21618.1_Listeria_monocytogenes (167) RILASIMMLFGIAFIGMITSTITNFFRAKKP----------
NP_631700.1_Streptomyces_coelicolor (89) RLVAVVVMVAGITSFGLVTAALATWFVG-------------
WP_006887331.1_Rothia_aeria (215) RVIAVVVMIYGVGLFGVITGALATWVIEKISGV--------
Consensus (616) RIVGIL IIAGI IAL V I S F

Figure 4

Structural validation.

A. Normalized QMEAN score of theoretical 3D structure for GiK protein model created with SWISS-MODEL server. **B.** Graphical representation of the Z-Score of the individual component of QMEAN. **C.** ProSA-web Z-scores of all proteins chains in PDB determined by X-ray crystallography (light blue) or NMR spectroscopy (dark blue). The Z score of GiK is highlighted as a black dot. **D.** Ramachandran plot analysis, 94.2% of total residues are in the most favored region.

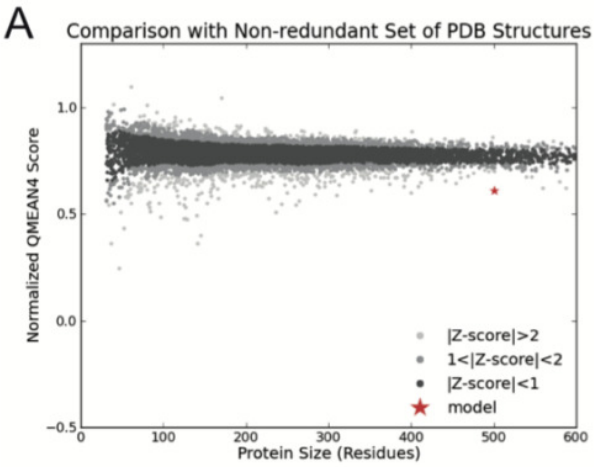
A
Comparison with Non-redundant Set of PDB Structures
Normalized QMEAN4 Score
Protein Size (Residues)
|Z-score|>2
1<|Z-score|<2
|Z-score|<1
model

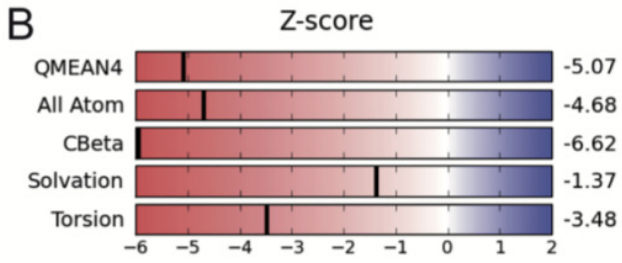
B
Z-score
QMEAN4
All Atom
CBeta
Solvation
Torsion
-5.07
-4.68
-6.62
-1.37
-3.48

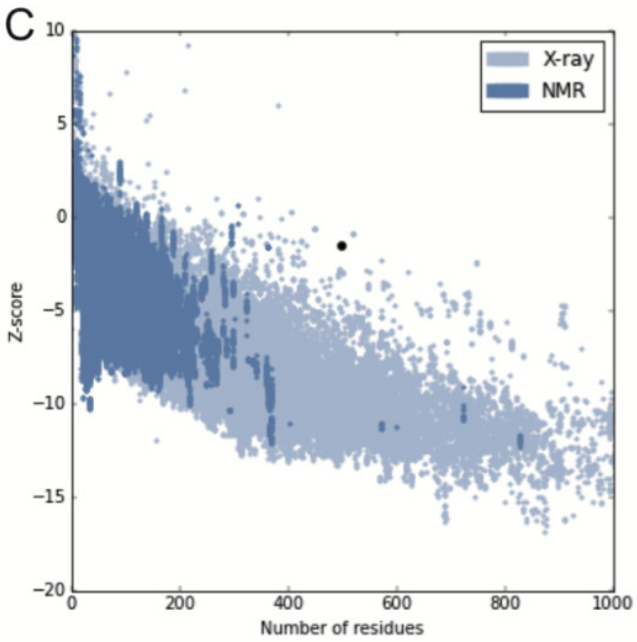
C
X-ray
NMR
Z-score
Number of residues

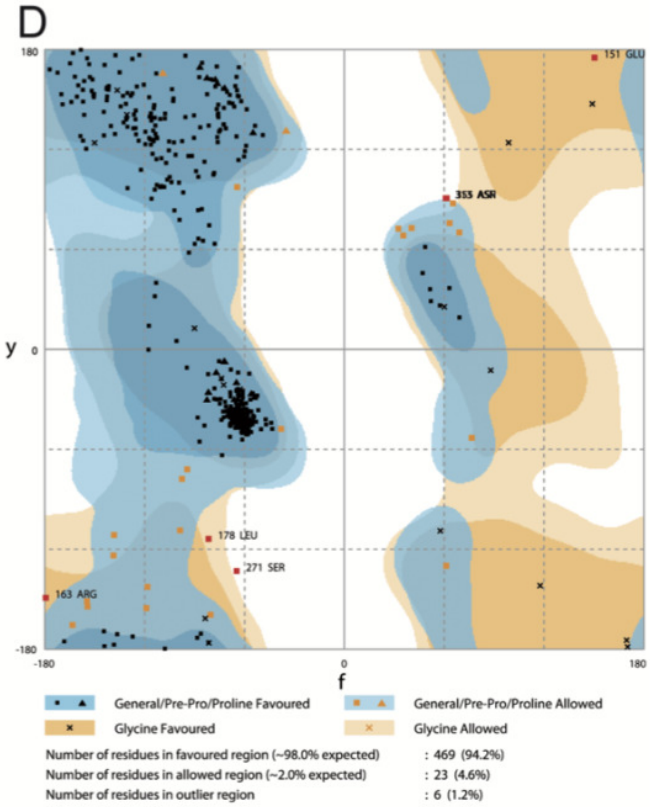
D
151 GLU
353 ASP
178 LEU
271 SER
163 ARG
y
f
General/Pre-Pro/Proline Favoured
General/Pre-Pro/Proline Allowed
Glycine Favoured
Glycine Allowed
Number of residues in favoured region (~98.0% expected) : 469 (94.2%)
Number of residues in allowed region (~2.0% expected) : 23 (4.6%)
Number of residues in outlier region : 6 (1.2%)

Figure 5

Quality estimation of GiK as a membrane protein.

Prediction done with SWISS-MODEL-QMEANBrane tool.

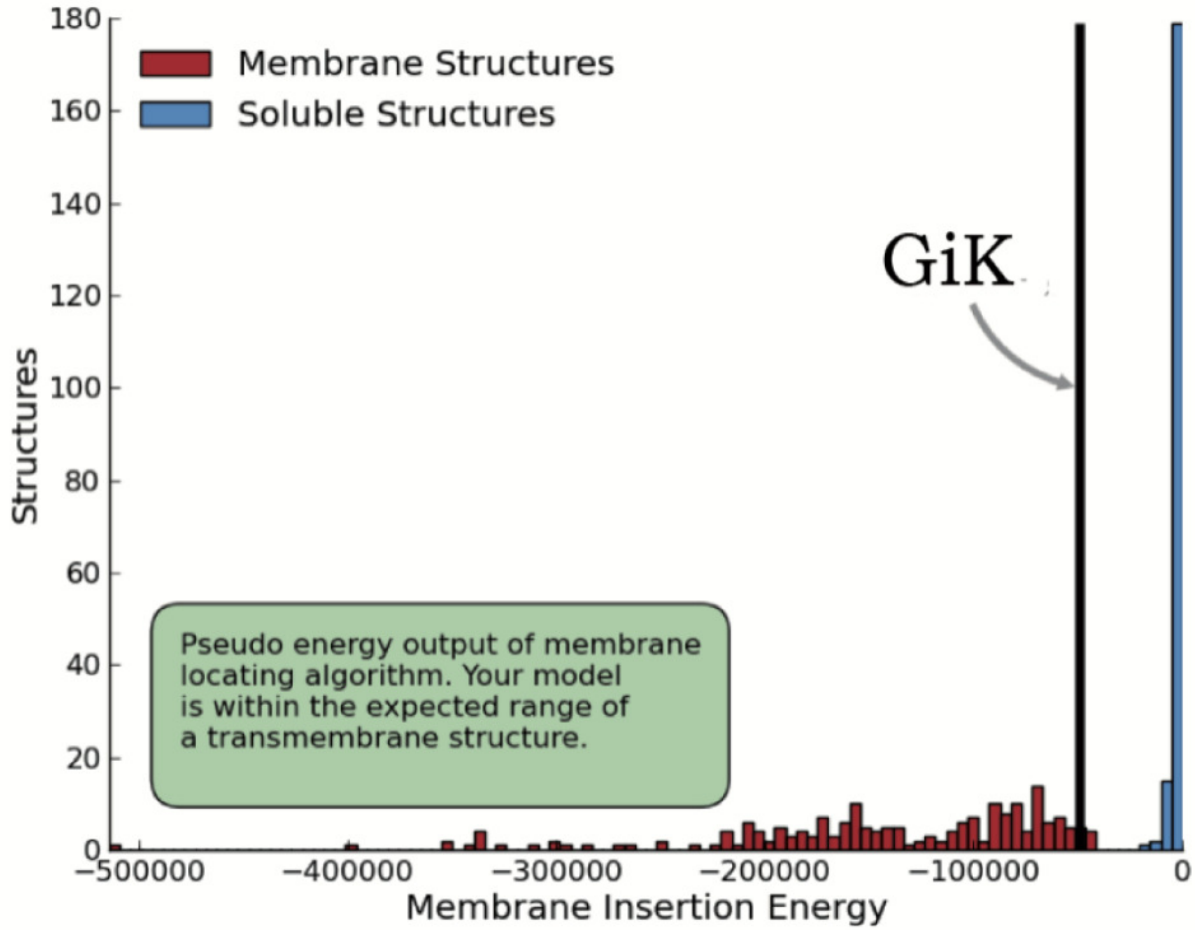
Membrane Structures
Soluble Structures
GiK
Structures
Membrane Insertion Energy
Pseudo energy output of membrane locating algorithm. Your model is within the expected range of a transmembrane structure.
180
160
140
120
100
80
60
40
20
0
−500000
−400000
−300000
−200000
−100000
0

Figure 6

Representation of the 3D-GiK modelled structure.

A. Monomer, **B-C**. Tetramer. The images were generated using MAESTRO-I software.

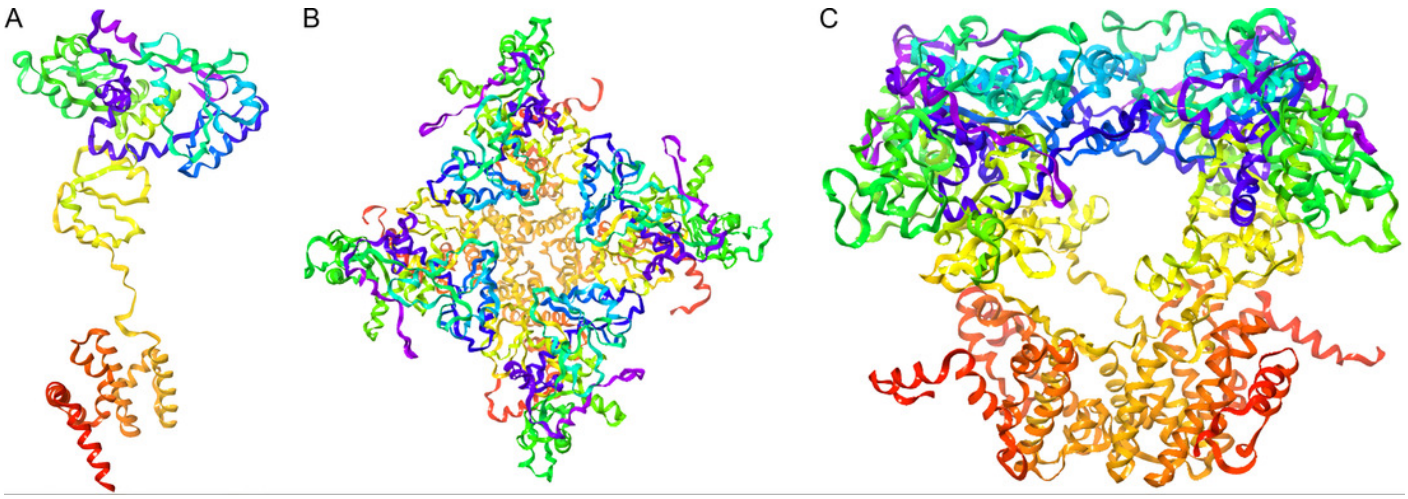

Figure 7

GiK - potassium channel blockers docking simulations (A).

B-D. Magnified views of the boxed regions depict the three potassium blockers channels binding sites (blue region I, red region II and green region III).

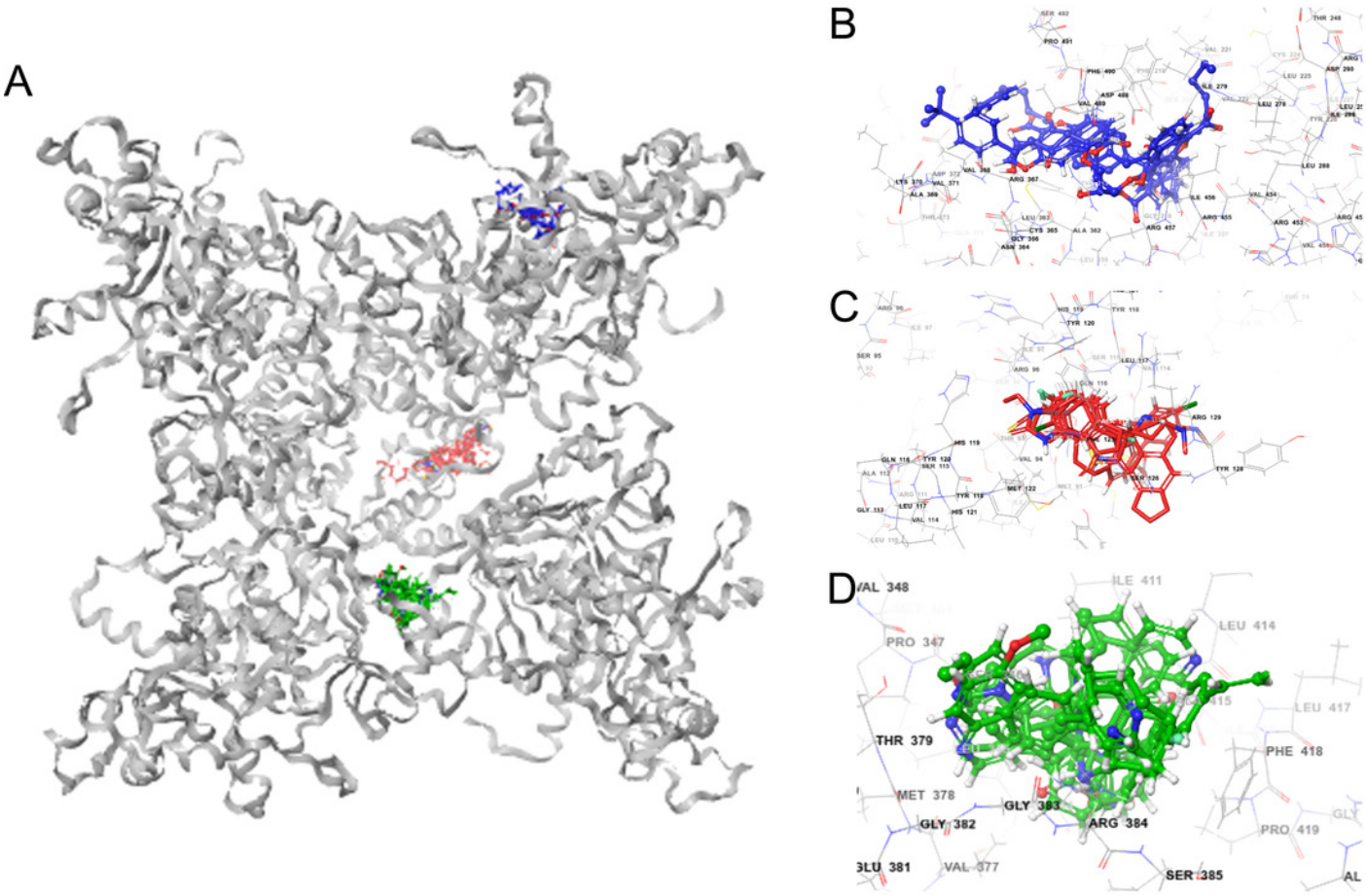

Figure 8

Ligand interaction diagrams.

UCL 1684 (A), Bicuculline (B) or verruculogen (C). Hydrophobic interactions are depicted by green curves, pi–pi interactions are in green-dashed lines, and the polar interactions by curve blue lines.

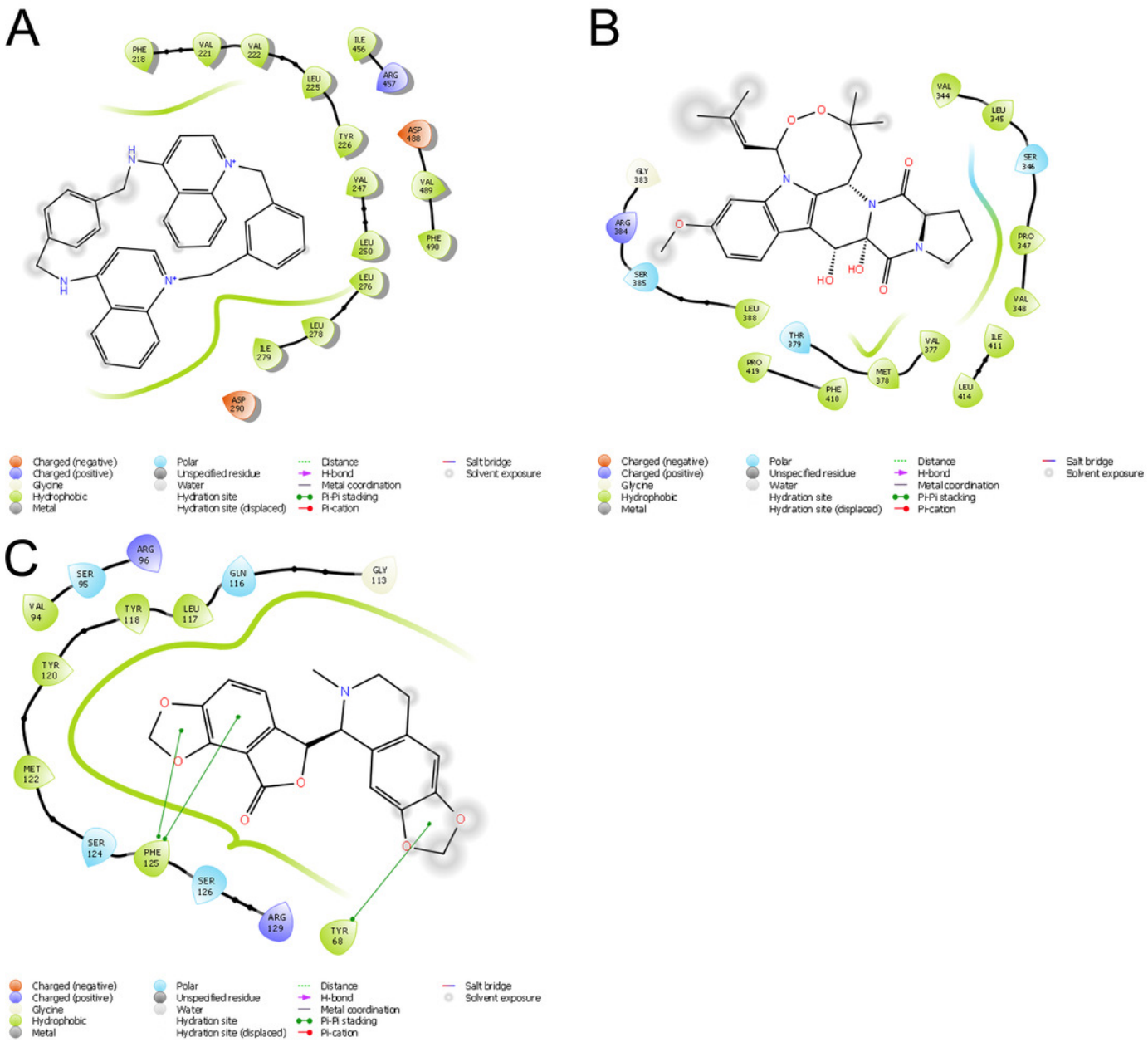

Table 1(on next page)

Sequences producing significant alignments with GiK by BLAST.

Accession number	Organism	Type of channel	Score	E. value	Identities	Positives
WP_022541369.1	*Aeropyrum camini*	Kv	32	0.33	15/49 (31%)	29/49 (59%)
AEE68730.1	*Bordetella pertussis*	Kv	32	0.51	15/43 (35%)	25/43 (58%)
YP_001776865.1	*Burkholderia cenocepacia*	Kv	33	0.20	16/39 (41%)	25/39 (64%)
YP_002407586.1	*Escherichia coli*	Kv	28.9	8.6	18/66 (27%)	36/66 (55%)
WP_024212520.1	*Escherichia spp*	Multispecies Kv	28.9	9.8	18/66 (27%)	36/66 (55%)
AAP94028.1	*Gallus gallus*	Kv1.3	34.7	0.27	20/58 (34%)	32/58 (55%)
YP_656932.1	*Haloquadratum walsby*	Kv	33	0.18	10/20 (50%)	18/20 (90%)
AAA61276.1	*Homo sapiens*	Kv	35	0.24	16/43 (37%)	25/43 (58%)
NP_002223.3	*Homo sapiens*	Kv1.3	35.0	0.17	20/58 (34%)	32/58 (55%)
CDS30290.1	*Hymenolepis microstoma*	Kv	32.7	2.4	22/80 (28%)	40/80 (50%)
AEO96823.2	*Lateolabrax japonicus*	Kv1.3	33.1	0.56	18/45 (40%)	26/45 (58%)
CCQ21618.1	*Listeria monocytogenes*	Kv	36	0.012	14/41 (34%)	27/41 (66%)
NP_001245037.1	*Macaca mulatta*	Kv1.3	35.0	0.18	20/58 (34%)	32/58 (55%)
NP_032444.2	*Mus musculus*	Kv1.3	33.5	0.47	14/38 (37%)	24/38 (63%)
XP_007383667.1	*Punctularia strigosozonata*	Kv	44	5e-04	33/105 (31%)	53/105 (50%)
WP_006887331.1	*Rothia aeria*	Kv	36.6	0.032	17/67 (25%)	34/67 (51%)
NP_707157.2	*Shigella flexneri 2a str. 301*	Kv	29	5.3	18/66 (27%)	36/66 (55%)
CAA56175.1	*Solanum tuberosum*	Kir	32.0	1.9	18/67 (27%)	34/67 (51%)
NP_631700.1	*Streptomyces coelicolor*	Kv	30	0.54	9/34 (26%)	24/34 (71%)
CDW52461.1	*Trichuris trichiura*	Kv	31.6	1.9	12/49 (24%)	27/49 (55%)
WP_033004452.1	*Vibrio azureus*	Kv	31.6	1.3	27/91 (30%)	46/91 (51%)

1

Table 2(on next page)

Physicochemical characterization of GiK by Protparam .

Number of amino acids	1416
Molecular weight	25811.2
Instability index	45.47
Aliphatic index	93.28
Grand average of hydropathicity (Gravy)	-0.053
Isoelectric point	8.18
Ext. Coeficiente	141880

1

Table 3(on next page)

Prediction of highly conserved residues from GiK.

Domain or motif	Description	Accession number	Position (E value)	Server
Ion_trans_2	Ionic channel. This family includes the two membrane helix type ion channels found in bacteria.	pfam07885	168-245 (1.35e-08)	NCBI Conserved domains, Motif Search, InterProScan tool
227696	EXS domain-containing protein [Signal transduction mechanisms].	COG5409	12-170 (0.44)	ExPASy PROSITE, Motif Search
215625	Voltage-dependent potassium channel; Provisional.	PLN03192	181-242 (0.14)	ExPASy PROSITE, Motif Search
236711	Voltage-gated potassium channel; Provisional.	PRK10537	196-214 (0.70)	ExPASy PROSITE, Motif Search
2POREKCHANEL	Potassium channel domain	PR01333	202-230 (0.00032)	Block Searcher
EAGCHANLFMLY	EAG/ELK/ERG potassium channel family signature	PR01463	193-210 (0.029)	Block Searcher
KCHANNEL	Potassium channel signature	PR00169	190-212 (0.1)	Block Searcher

1

Table 4(on next page)

Validation scores from RAMPAGE, QMEAN, ProSA-web, ERRAT and Verify 3D of the constructed models.

1

Software	Templete (PDB ID)	Ramachandran (%)	QMEAN score	Z-score	ERRAT score	Verify 3D	Residues	RMSD (Å)
Modeller	5TJ6	90.4	0.141	-7.56	44.26	26.28	500	4.28
	5U70	90.0	0.094	-8.09	39.62	14.06	500	5.05
	5TJI	94.2	0.296	-5.07	69.24	35.60	500	3.90
	5U76	88.4	0.023	-9.22	34.97	26.28	500	4.46
Raptorx	5TJ6	89.8	0.191	-6.92	56.64	20.60	500	4.85
I-tasser	5TJ6	72.9	0.101	-8.78	86.58	38.80	500	3.97
	5U70	69.6	0.089	-9.12	81.91	44.60	500	5.01
Swiss model	5TJ6	89.8	0.205	-6.21	81.48	33.00	296	0.92
	5U70	92.8	0.271	-5.53	87.54	39.38	292	0.91
	5TJI	92.5	0.240	-5.82	88.57	30.98	296	1.12
	5U76	92.9	0.191	-6.34	84.17	26.35	297	1.17
Phyre2	5TJ6	95.7	0.239	-5.72	61.63	37.36	265	1.01
	5U76	94.7	0.251	-5.99	35.04	38.44	372	1.10

2

Table 5(on next page)

Best docking score values (kcal/mol) from the potassium channel blockers to 3D-GiK model.

Compound	Docking score (kcal/mol)	Compound	Docking score (kcal/mol)	Compound	Docking score (kcal/mol)
UCL_1684	-11.2	ZINC13489790	-8	Flecainide	-6.9
ZINC38144725	-10.8	Imipramine	-7.9	Mepivacaine	-6.9
Terfenadine	-10.6	Trifluoroperazine	-7.9	ZINC13489786	-6.8
ZINC00018512	-10.4	ZINC13489791	-7.9	ZINC13760202	-6.8
ZINC00598948	-10.1	ZINC13489800	-7.9	ZINC13777065	-6.8
Bicuculine	-10	ZINC13489804	-7.9	1-Ethyl-2-Benzimidazolinone	-6.7
Cromoglicic acid	-10	ZINC13489830	-7.9	ZINC13760207	-6.7
Penitrem_A	-10	ZINC13760212	-7.9	ZINC13760214	-6.7
BMS_204352	-9.4	Linopirdine	-7.8	ZINC03935230	-6.5
NS1643	-9.1	ZINC13442157	-7.8	ZINC13557606	-6.5
Paxilline	-9.1	ZINC13489810	-7.8	ZINC13777062	-6.5
CP_339818	-9	ZINC13489818	-7.8	ZINC27617403	-6.5
Tubocurarine	-8.9	ZINC13489829	-7.8	Dofetilide	-6.4
ZINC13489797	-8.8	ZINC13489785	-7.7	Retigabine	-6.4
UK_78282	-8.7	TRAM_34	-7.6	ZINC00005768	-6.4
Verruculogen	-8.7	ZINC13489794	-7.6	ZINC13760203	-6.4
ZINC13489806	-8.6	ZINC13489798	-7.6	ZINC13777063	-6.4
ZINC13644028	-8.6	ZINC13489784	-7.5	ZINC13777067	-6.4
DIDS	-8.5	ZINC13489803	-7.5	Correolide	-6.3
ZINC01535217	-8.5	ZINC13489813	-7.5	ZINC03935234	-6.3
ZINC13442159	-8.5	ZINC13557604	-7.5	ZINC03935235	-6.3
ZINC38144724	-8.5	Amitriptyline	-7.4	ZINC03946466	-6.3
Bicuculine methiodide	-8.4	Dequalinium	-7.4	ZINC13777069	-6.3
ZINC13489814	-8.4	ZINC01539875	-7.4	ZINC13777072	-6.3
ZINC13489817	-8.4	ZINC13489789	-7.4	Procaine	-6.2
ZINC00015850	-8.3	Quinidine	-7.3	Zoxazolamine	-6.1
ZINC00603820	-8.3	ZINC00014006	-7.3	ZINC13777058	-6
ZINC01539867	-8.2	ZINC01535218	-7.3	ZINC18096411	-6
ZINC13489795	-8.2	ZINC13760206	-7.3	ZINC13777075	-5.8
ZINC13489796	-8.2	ZINC27617400	-7.3	ZINC13643922	-5.7
ZINC13489807	-8.2	Psora_4	-7.2	Chlorzoxazone	-5.5
ZINC13489823	-8.2	ZINC18189761	-7.2	ZINC13579814	-5.5
ZINC29309163	-8.2	Pimaric_acid	-7.1	LY_97241	-5
Niguldipine	-8.1	Miconazole	-7	Clofilium	-4.8
ZINC13489799	-8.1	ZINC13760204	-7	Halothane	-4.5
XE991	-8	ZINC13760205	-7	4_Aminopyridine	-4.4
ZINC01539870	-8	ZINC13760213	-7		

1

Table 6(on next page)

Binding sites from the potassium channel blockers to GiK.

Region	Amino acid residues	Potassium channel blockers
I	Phe218, Val221, Val222, Leu225, Tyr226, Leu250, Leu278, Ile279, Ile456, Arg457, Asp488, Val489, Phe490	UCL_1684, terfenadine, cromoglicic acid, CP_339818, niguldipine, imipramine, Psora_4, mepivacaine, procaine, chlorzoxazone, 4_Aminopyridine
II	Leu65, Gly113, Gln116, Leu117, Tyr120, Met122, Phe125, Ile127, Arg129	Bicuculine, Penitrem_A, BMS_204352, NS1643, paxilline, tubocurarine, UK_78282, DIDS, bicuculine methiodide, trifluoroperazine, amitriptyline, dequalinium, miconazole, flecainide, 1-Ethyl-2-Benzimidazolinone, correolide, clofilium, halothane
III	Val344, Leu345, Ser346, Val377, Thr379, Gly383, Arg384, Leu388, Leu414, Ala415, Phe418, Pro419	Verruculogen, XE991, linopirdine,TRAM_34, quinidine, pimaric_acid, dofetilide, retigabine, zoxazolamine ,LY_97241

1